1955

Nonlinear capacitor control of a swept frequency generator.

Williams, Buck D.

Monterey, California: U.S. Naval Postgraduate School

NONLINEAR CAPACITOR CONTROL OF A SWEPT FREQUENCY GENERATOR

BUCK D. WILLIAMS, JR.

NONLINEAR CAPACITOR CONTROL OF A SWEPT FREQUENCY GENERATOR

* * * * * *

Buck D. Williams, Jr.

NONLINEAR CAPACITOR CONTROL OF A SWEPT FREQUENCY GENERATOR

by

Buck Daniel Williams, Jr.
Lieutenant, United States Navy

Submitted in partial fulfillment
of the requirements
for the degree of
MASTER OF SCIENCE
IN
ENGINEERING ELECTRONICS

United States Naval Postgraduate School
Monterey, California

1955

This work is accepted as fulfilling

the thesis requirements for the degree of

MASTER OF SCIENCE

IN

ENGINEERING ELECTRONICS

from the

United States Naval Postgraduate School

PREFACE

During World War II, a shortage of mica led investigators to study the dielectric properties of other materials. One of the materials investigated was barium titanate. This material proved to have an extremely high dielectric constant which varies with applied voltage and may be used as a non-linear circuit element.

It is the objective of this thesis to develop a wide range swept frequency radio frequency generator. In the development of this swept frequency generator, the variation of dielectric constant (capacity) of barium titanate is utilized to form a voltage tuneable frequency determining circuit. To predict the behavior of the swept frequency generator, equations are derived from experimental measurements of capacity of a barium titanate capacitor which express the capacity as a function of applied voltage and which describe the capacitor voltage as a function of time when placed in a network in which direct and alternating voltages are applied.

It is proposed that the non-linear variation of capacity with voltage of a barium titanate capacitor may be used to advantage in generating wave forms of various shapes when placed in a series charging circuit consisting of a linear resistor, nonlinear capacitor and a battery. Practical applications for the various wave forms are found in the swept frequency generator and in other circuits. It is further proposed that the use of barium titanate in a wide range swept frequency generator is a natural application of this material since the swept frequency generator uses changes in capacity with bias voltage which are of such a large

magnitude that variations in capacity due to other factors, such as temperature and age, are not significant.

The writer wishes to thank Professors Carl E. Menneken, Earl G. Goddard and P. E. Cooper, all of the U. S. Naval Postgraduate School, for their assistance, encouragement and cooperation in the preparation of this paper.

TABLE OF CONTENTS

LIST OF ILLUSTRATIONS

Figure Page

TABLE OF SYMBOLS AND ABBREVIATIONS

(Listed in the order of their use in text)

1. VHF - Very High Frequency
2. D. C. - Direct Current
3. C_o - A constant having the dimensions of farads
4. k - A constant having the dimensions of farads/volt
5. V_c - D. C. voltage across a condenser
6. C_1 - A constant having the dimensions of farads
7. α - A constant having the dimensions of 1/volt
8. i - instantaneous current, amperes
9. t - Time, seconds
10. V_o - Battery voltage in a series charging network
11. RC - Resistance-capacitance
12. RF - Radio-frequency

CHAPTER I

INTRODUCTION

1. SWEPT FREQUENCY OSCILLATORS

Swept frequency oscillators are oscillators whose output frequency varies as some function of time. They are useful in such applications as the measurement of the frequency response of various electronic circuits and as an integral part of such devices as panoramic adapters.

The basic principle upon which swept frequency oscillators operate is that an element, or elements, in the frequency determining tank circuit of an oscillator may be made to vary with the time and hence the frequency of the output voltage of the oscillator will also vary with the time.

Wide frequency bands may be covered in one sweep by beating a fixed frequency oscillator with a swept high frequency oscillator which is swept over a small portion of the high frequency band. The difference in the two frequencies is obtained from an electronic mixer and the difference frequency then covers many octaves of a much lower frequency band.

The most stable swept frequency oscillator is one with a frequency determining circuit made up of conventional components. One component in this circuit, usually a variable air dielectric condenser, is varied by a motor drive. These oscillators may be made as stable and accurate as a conventional standard frequency oscillator. The difference in operation lies in the fact that the motor drive tunes the oscillator through its useful range in a very short time.

Reactance tubes are convenient up to the very high frequency range and may be used to control the frequency of an oscillator over a fraction of the center frequency of the oscillator.

A wide band swept frequency generator has been developed at medium frequencies using a nonlinear inductor in the frequency determining circuit of the oscillator. The inductance in the tank circuit is varied by the amount of D.C. current flowing through the nonlinear inductor.

Voltage tuned klystron oscillators are now in use as swept frequency oscillators in the micro-wave range and are also used in mixer circuits to obtain the difference frequency between the swept klystron and a fixed tuned oscillator (which may be another klystron). The difference frequency may be made to cover a wide range in a lower frequency band such as the VHF band.

A new development may soon make available a stable swept frequency oscillator which will cover the entire audio range of 20 to 20,000 cycles per second in one sweep. The Hewlett-Packard Company has developed a method of synthesizing an impedance which has a constant phase angle, but whose magnitude varies as a negative power of frequency. By replacing the two resistors in a standard Wien Bridge Oscillator with two impedance elements such as described above it is possible to obtain an oscillator circuit whose output frequency is equal to a constant times the value of the Wien Bridge Oscillator tuning condenser to the negative third power. Varying the tuning condenser over a 10 to 1 capacity range then varies the output frequency over a 1000 to 1 frequency range. The tuning condenser is a standard air dielectric condenser and may be varied by a motor control which results in a stable audio frequency swept frequency

oscillator.

The nonlinear variation of capacity versus D.C. bias voltage of Barium Titanate capacitors offers a method of designing a swept frequency oscillator in which the Barium Titanate capacitor is used as the tuning element in the oscillator tank circuit.

2. BARIUM TITANATE

The material used as the dielectric in the fabrication of the non-linear capacitors used in the experimental investigations connected with this paper is barium titanate. Barium titanate is a member of a group of about 25 ferroelectric materials. As described by W. P. Mason and R. F. Wick [4]*

> Ferroelectric materials are the dielectric analog of ferromagnetic materials. Their uses parallel those of ferromagnetic materials in such applications as high permeability materials, magnetostrictive transducers, magnetic amplifiers, and magnetic information storage devices.

In a recent book, "Dielectrics and Waves", A. R. von Hippel [6] devotes a chapter to "Ferroelectricity" in the second part of the book entitled "Molecular Approach". The crystalline and molecular properties of barium titanate are described and numerous references are given to detailed descriptions in the literature.

A review of the measured properties of single crystals of barium titanate is made by W. P. Mason and R. F. Wick [4]. Also methods of stabilizing characteristics of ceramics of barium titanate by certain additives and aging by heat treatment are described.

In a series of articles, A. I. Dranetz, G. N. Howatt and J. W. Crownover [2] give a general description of the known properties of barium titanate and barium titanate ceramics and the practical applications

* Numerals in brackets indicate the number of a reference listed in the bibliography

of these dielectrics. Also included are references to many detailed treatments in the literature.

At certain temperatures, barium titanate exhibits an extremely high dielectric constant which varies with temperature. For pure barium titanate the dielectric constant shows an extremely high and sharp peak at 120 degrees centigrade. This is a Curie temperature above which barium titanate has a cubic structure and below which the structure is tetragonal. Other, but less marked transitional temperatures occur at plus 10 and minus 70 degrees centigrade. Measurements have shown that the dielectric constant of barium titanate varies with a D. C. bias voltage across the dielectric. This variation of dielectric constant is noticeable below and above the Curie temperature. Accompanying this variation of dielectric constant with voltage is a hysteresis effect. For pure barium titanate crystals the hysteresis loop is nearly square below the Curie temperature and varies in area with bias voltage. The area of the hysteresis loop becomes small above the Curie temperature. Barium titanate may also be made piezoelectric below the Curie temperature by proper processing of the material.

Ceramics of barium titanate may be made by sintering together many crystals. These ceramics have much the same properties as the single crystal and can be formed in any desired shape and size.

Certain additives may be added to the ceramics of barium titanate to modify its properties so that it may meet the needs for various applications. The Curie temperature has been found to vary linearly with the amount of strontium titanate added. By the proper addition of strontium titanate, the Curie temperature may be lowered to a desired temperature.

Considerable variations in dielectric constant and power factor are found at room temperature due to the presence of the second transition. These properties may be stabilized by the addition of lead and calcium titanates which lower the second transition temperature. Lead titanate also raises the Curie temperature while calcium titanate leaves the Curie temperature unchanged. Hence, considerable variation of the properties of barium titanate may be achieved.

Dranetz, Howatt, and Crownover, [2] describe the use of barium titanate in electro-acoustic devices which utilize the piezoelectric effect; in capacitors and delay lines which utilize the high dielectric constant; in temperature sensitive devices which utilize a constant temperature coefficient of capacity over wide ranges of temperature for certain titanate bodies; and in frequency modulation and dielectric amplifiers which utilize the change in capacity with bias voltage.

Mason and Wick, [4] describe many of the above applications as well as that of information storage devices and a dielectric amplifier which utilize the square hysteresis loop of single crystals below the Curie temperature. The amplifier described by Mason and Wick utilizes a carrier frequency of 200 kilocycles and yields a gain of 12 decibels for signal frequencies of zero to 7000 cycles per second.

In a recent article, G. S. Shaw and J. L. Jenkins, [5] describe several commercial dielectric amplifier capacitors and their use in a dielectric amplifier giving an output of 300 milliwatts from a 0.3 milliwatt signal source.

A recent development in frequency modulation is described by Maurice Apstein and H. H. Wieder, [1] in which a barium titanate

capacitor was coupled into an oscillator tank circuit to give frequency modulation deviations of plus and minus two percent of the carrier frequency in the range of 50-500 megacycles per second.

CHAPTER II

THEORY OF THE CHARGE OF NON-LINEAR CAPACITORS

Figure 1 shows the capacity versus D. C. bias characteristics of a capacitor made from a small slab of GLENCO type K-6000 barium titanate. The sample K-6000 was selected over several other types tested due to a larger variation in capacity per unit variation in bias voltage. The circuit used to measure the characteristics of this sample is shown in the figure. Not shown in the figure is the behavior of this sample when the bias voltage is reversed. Reversal of the bias voltage gives rise to a slight dielectric hysteresis loop which will affect the discharge characteristics of the sample. In the swept frequency generator developed, only the charge characteristics of the dielectric is used over a large change in voltage and hence only the curve for the charge of the capacitor is included. The hysteresis effect will, of course, cause some loss in the frequency determining circuit of the oscillator, but the peak to peak variation of the radio frequency voltage in the frequency determining circuit will, in general, be small in comparison to the D. C. bias voltage across the dielectric.

In order to develop the equations which describe the behavior of the non-linear capacitor during the charging period, equations which describe the small signal capacity, or the differential capacity, as a function of bias voltage must first be obtained. Since the differential equations which will have to be solved will have variable coefficients and will be difficult to solve exactly in many cases, care must be exercised in selecting the empirical expressions used to describe the variation of

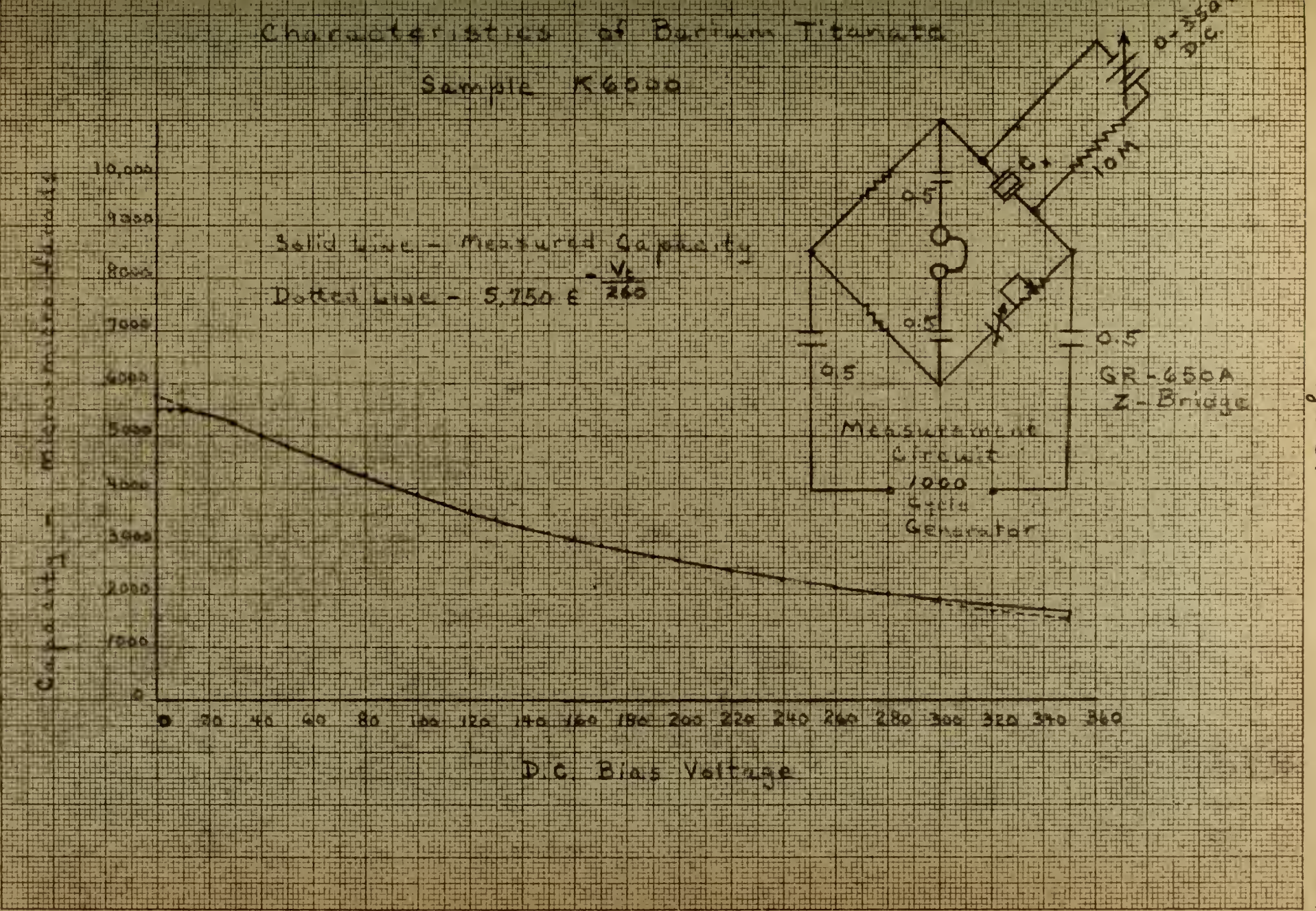
Characteristics of Barium Titanate
Sample K6000
Solid Line - Measured Capacity
Dotted Line - $5,750\ \epsilon^{-\frac{V_c}{260}}$
Capacity in μμf
10,000
9000
8000
7000
6000
5000
4000
3000
2000
1000
0
0 20 40 60 80 100 120 140 160 180 200 220 240 260 280 300 320 340 360
D.C. Bias Voltage
0-350 D.C.
0.1
10M
0.5
0.5
0.5
0.5
GR-650A
Z-Bridge
Measurement
Circuit
1000
Cycle
Generator

Figure 1

capacity with voltage. Two expressions for capacity as a function of voltage, which are accurate over certain ranges of voltage for the capacitor of figure 1, readily lead to differential equations whose solutions may be easily obtained, and values of capacitor voltage versus time during the charge period may be found tabulated in mathematical tables. These two expressions are:

(1) $$C = C_o - kV_c \qquad (2.01)$$

where: V_c = voltage across the capacitor

and : $V_1 < V_c < V_2$

This expression is exact, of course, for only two points on the characteristic curve; however, any curve may be divided into many small segments, each segment of which will have its own value of C_o and k.

(2) $$C = C_o + C_1 \epsilon^{-\alpha V_c} \qquad (2.02)$$

where: V_c = voltage across the capacitor

and : $V_1 < V_c < V_2$

The above expression, while exact for only three arbitrary points, has been found to be in error by only a few percent over wide changes in voltage for the sample whose characteristics are shown in figure 1.

If three points are chosen on the characteristic curve of capacity versus voltage so that:

$$C = C_a \quad \text{when} \quad V_c = V_a \qquad (2.03)$$

$$C = C_b \quad \text{when} \quad V_c = V_b \qquad (2.04)$$

$$C = C_d \quad \text{when} \quad V_c = V_d \qquad (2.05)$$

and:

$$V_b - V_a = V_d - V_b \qquad (2.06)$$

values of C_o, C_1 and α are readily obtained by substitution into the above equation.

Figure 2 shows a hypothetical non-linear dielectric capacitor, C, connected in series with a linear resistor, R, and a D. C. source of potential of value V_o. Figure 2 shows the assumed variation of capacity with voltage which is represented by the equation:

$$C = C_o - K V_c \qquad \text{where} \quad K = \frac{C_o}{V_m} \tag{2.01}$$

where C_o is the intercept on the capacity axis and V_m is the intercept on the voltage axis.

The differential equation which describes the expected behavior of the circuit of figure 2 during the charge period is:

$$i = \frac{V_o - V_c}{R} = C \frac{dV_c}{dt} = (C_o - K V_c) \frac{dV_c}{dt} \tag{2.07}$$

The solution of equation (2.07) is obtained in Appendix I and is found to be:

$$t = RC_o \left[\frac{V_c - V_1}{V_m} + \left(1 - \frac{V_o}{V_m}\right) \ln \frac{V_o - V_1}{V_o - V_c} \right] \tag{2.08}$$

where: $V_1 \leq V_c \leq V_m$

Equation (2.08) may be compared with the equation for the charge time for a conventional capacitor by allowing V_m to approach infinity:

$$t = RC_o \ln \frac{V_o - V_1}{V_o - V_c} \tag{2.09}$$

It will be noted that when V_o is less than V_m equation (2.08) approaches (2.09) and the curve of capacitor voltage versus time will be

Figure 2

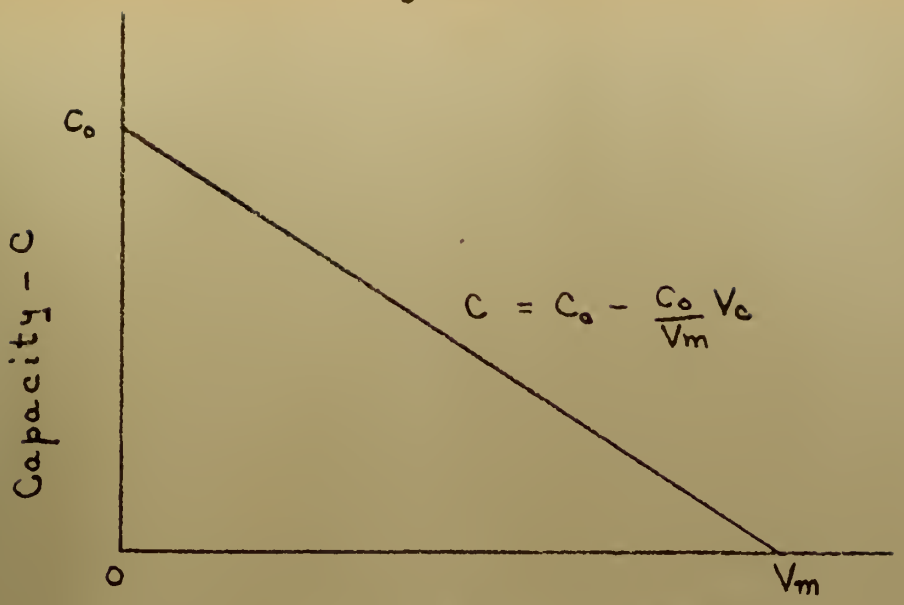

Assumed Characteristics
of Non-Linear Capacitor

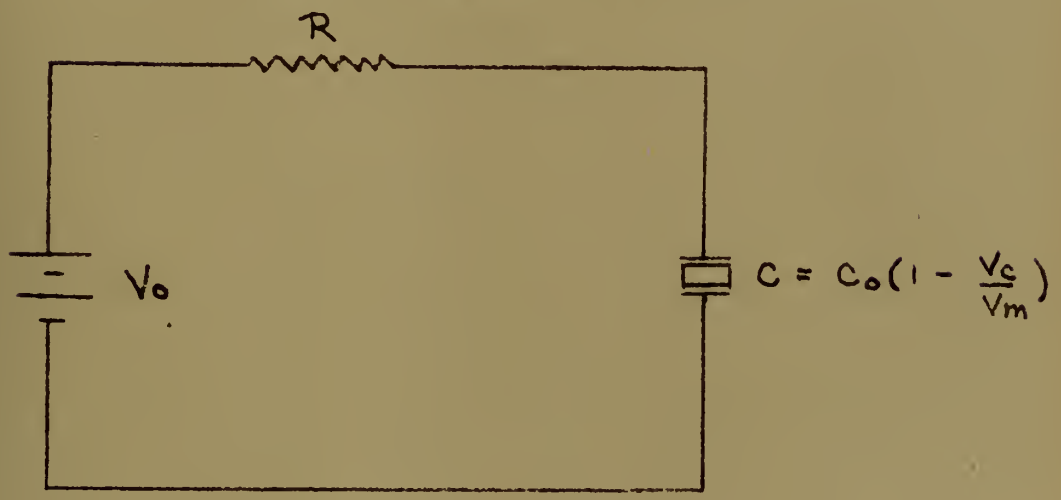

Charging Circuit

very similar to that of a conventional capacitor.

An interesting result of equation (2.08) is obtained by allowing V_o to approach V_m. In this case equation (2.08) becomes linear and the curve of capacitor voltage is predicted to be linear with time:

$$V_c = V_i + V_m \frac{t}{RC_o} \qquad (2.10)$$

When V_o is made greater than V_m, equation (2.08) predicts that the time required to charge to a given percentage of V_o is less the larger V_o is made. This is in contrast to the action of a conventional capacitor used in the circuit. For a conventional resistor-capacitor charge network the time to charge from zero to a given percentage of the battery voltage is the same for all battery voltages. The curve of capacitor voltage versus time for the non-linear capacitor when V_o is larger than V_m is thus concave upward, rather than downward as with the conventional capacitor, up to the point where V_c is equal to V_m which represents a point of discontinuity.

That the above equation (2.09) describes the variation of voltage across the capacitor may be verified in an RC charging network shown in figure 3. In this circuit the voltage across the capacitor of figure 1 is limited to that portion of the characteristic curve which is nearly linear. V2 sets the upper capacitor voltage limit and V3 sets the lower capacitor voltage limit. The results are observed on an oscilloscope.

Practical application of the linear change in capacitor voltage with time predicted by equation (2.10) may be found in oscilloscope sawtooth wave sweep circuitry and in timing circuitry.

To predict the behavior of the voltage across the capacitor whose

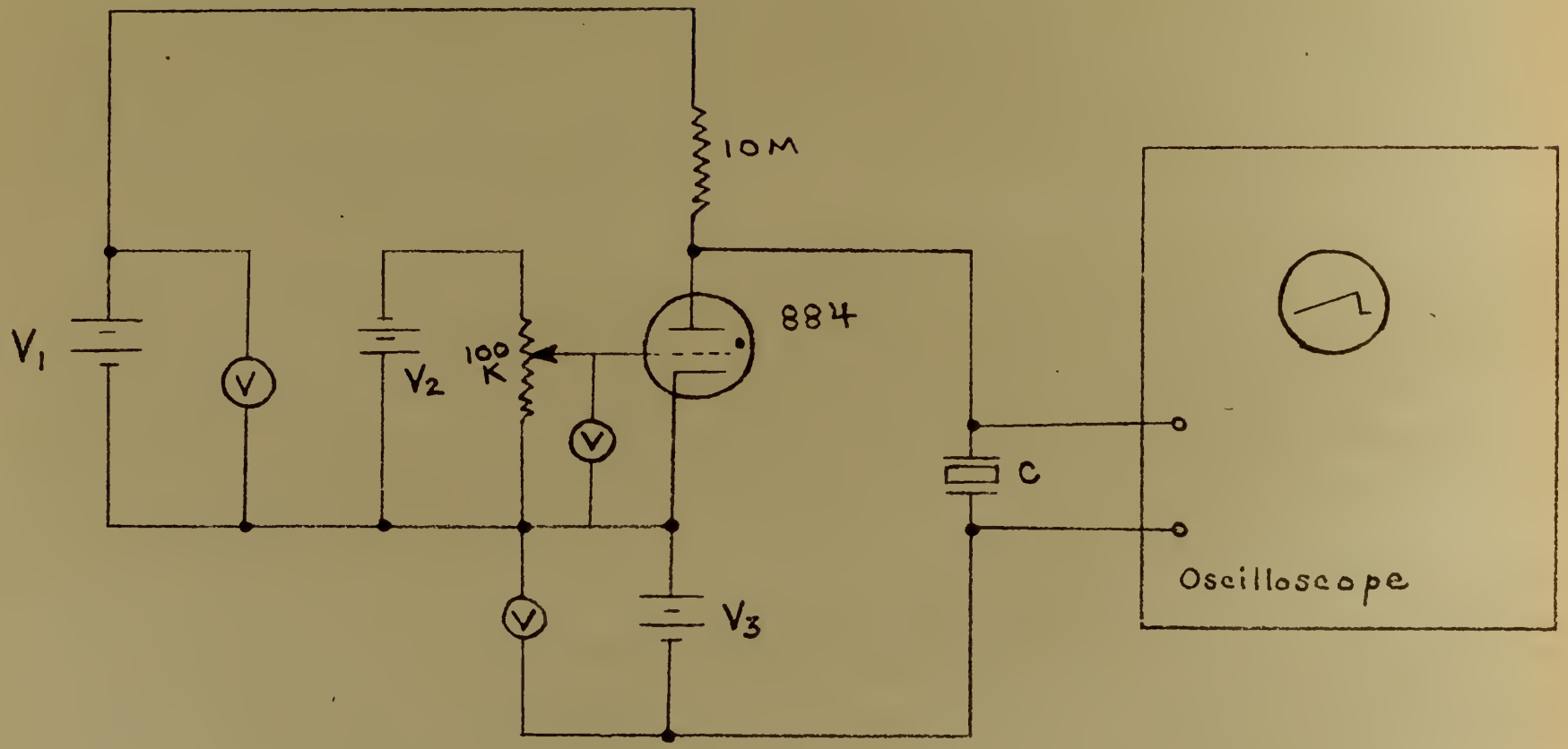

Figure 3

Circuit for Observing Charge Characteristics of Non-Linear Capacitor

characteristics are shown in figure 4, the curve is divided into several linear portions from V_1 to V_2; values of delta time are obtained for each portion of the curve from the following equation:

$$\Delta t = RK(V_2 - V_1) + R(KV_o - C_o) \ln \frac{V_o - V_1}{V_o - V_2} \qquad (2.11)$$

where a C_o and k are computed for each straight line segment; and all values of delta t are summed from zero to time t to provide points for plotting a curve of voltage versus time.

Curves derived from equation (2.11) for the capacitor of figure 1 will be similar to those of figure 6 which is plotted from equations derived in a later section. The curve for $\alpha V_o = 0.5$ corresponds to a battery voltage of 130 volts, the curve for $\alpha V_o = 1.0$ corresponds to a battery voltage of 260 volts and the curve for $\alpha V_o = 2.0$ corresponds to a battery voltage of 520 volts. It will be noted that over certain ranges of voltage the waveforms shown in figure 6 are similar to those predicted by equation (2.08).

J. R. MacDonald and M. K. Brachman, [3] discuss the behavior of a hypothetical exponential capacitor: $C_S = C_o \epsilon^{\alpha |V_c|}$. Equations are developed to describe the capacitor voltage as a function of time when placed in a series network with a resistor and a battery. This article has suggested that a negative exponential function may be used to describe the barium titanate capacitor of figure 1 which is to be used in the sweep frequency generator developed in connection with this thesis. This has proved to be more useful in this case than the method in which equation (2.11) is used. This usefulness is due to the fact it is possible to describe the behavior of the capacitor of figure 1 by a single

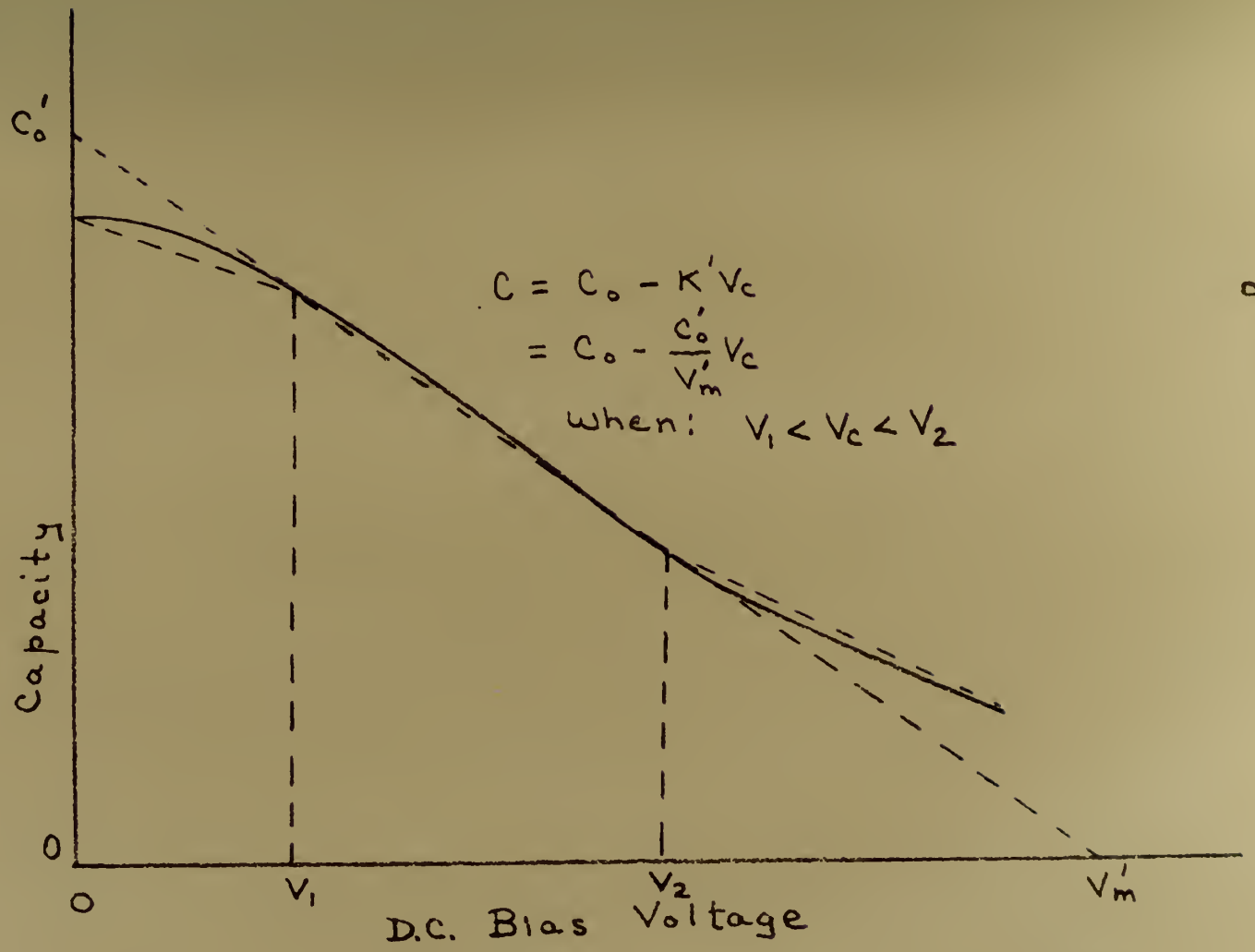

Figure 4

Characteristics of Non-linear Capacitor
Divided into straight Line Segments

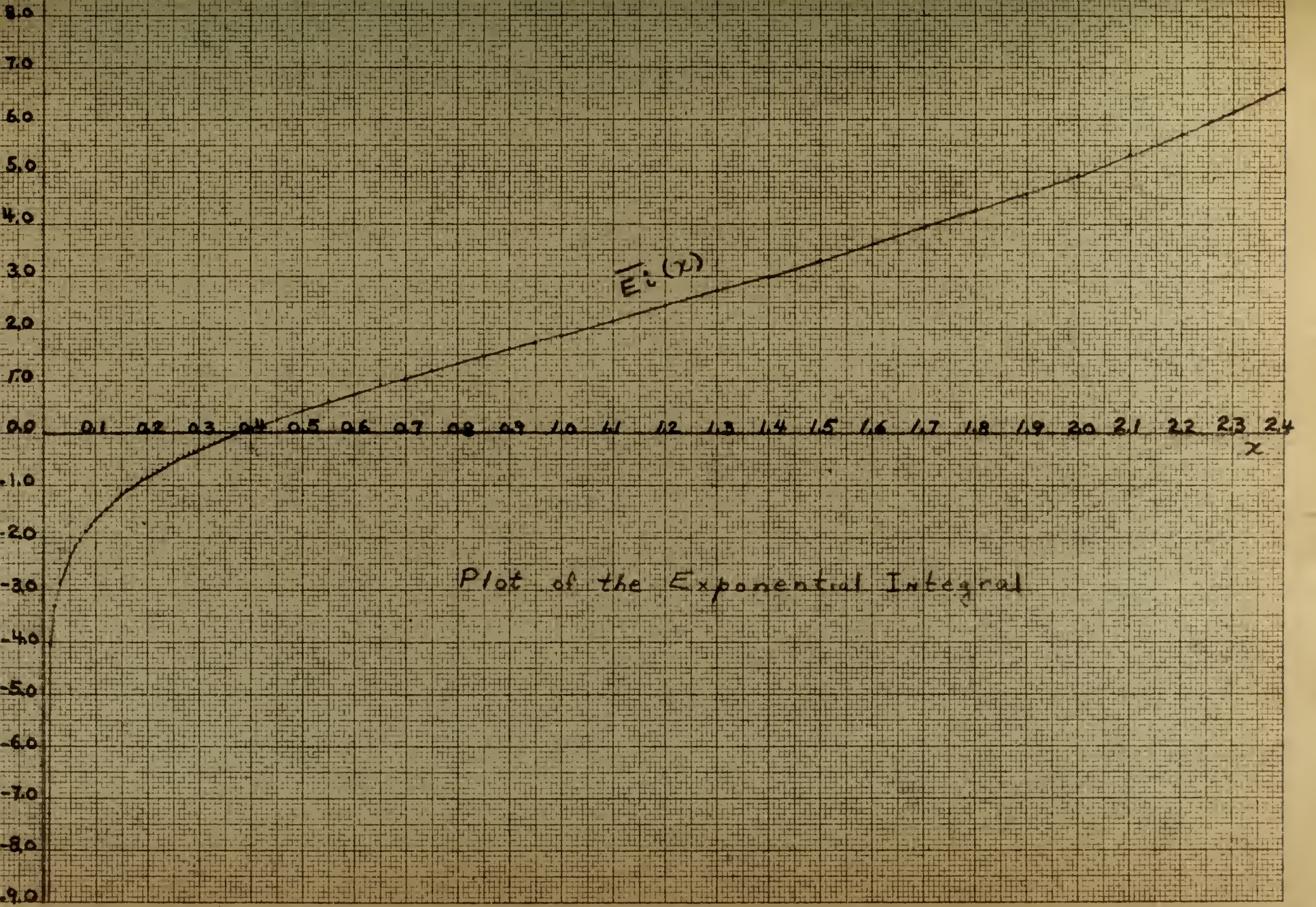
8.0
7.0
6.0
5.0
4.0
3.0
2.0
1.0
0.0
-1.0
-2.0
-3.0
-4.0
-5.0
-6.0
-7.0
-8.0
-9.0
0.1 0.2 0.3 0.4 0.5 0.6 0.7 0.8 0.9 1.0 1.1 1.2 1.3 1.4 1.5 1.6 1.7 1.8 1.9 2.0 2.1 2.2 2.3 2.4
x
$\overline{E}_1(x)$
Plot of the Exponential Integral

equation, $C = 5.75 \times 10^{-9} \epsilon^{-\frac{V_c}{260}}$, which is accurate within a few percent over very wide changes in capacitor voltage. In addition the solution of the resulting differential equation has been manipulated so that an integral evaluated graphically in the above article may be found readily in mathematical tables and will more rapidly yield curves of capacitor voltage versus time.

The differential equation for the negative exponential capacitor in a series RC circuit is:

$$\frac{V_o - V_c}{R} = \left(C_o + C_1 \epsilon^{-\alpha V_c}\right) \frac{dV_c}{dt} \qquad (2.12)$$

where: $C = C_o + C_1 \epsilon^{-\alpha V_c}$ (2.02)

and is solved in Appendix II.

The solution of the differential equation is:

$$t = R\left[C_o \ln \frac{V_o}{V_o - V_c} + C_1 \epsilon^{-\alpha V_o}\left\{\bar{Ei}[\alpha V_o] - \bar{Ei}[\alpha(V_o - V_c)]\right\}\right] \qquad (2.13)$$

In the solution in Appendix II integrals of the following type are evaluated:

$$I(\alpha V_o, \alpha V_c) = \int_{\alpha(V_o - V_c)}^{\alpha V_o} \frac{\epsilon^x}{x}\, dx \qquad (2.14)$$

The above integral is related to the integral:

$$J(\eta, \xi) = \int_{\eta - \xi}^{\eta} \frac{\epsilon}{y}^{-(\eta - y)}\, dy \qquad (2.15)$$

which has been integrated graphically by MacDonald and Brachman over useful ranges of the above limits of integration. By slight manipulation of the integral "J", it may be shown to be equal to the integral "I" times an exponential function. As is shown in Appendix II, the integral "I"

is equal to the difference in two tabulated values in Jahnke and Emde, "Tables of Functions", and can be readily evaluated without the labor involved in graphical integration:

$$J(\eta,\varepsilon) = \epsilon^{-\eta}\int_{\eta-\varepsilon}^{\eta} \frac{\epsilon^{y}}{y}\,dy = \epsilon^{-\eta}\int_{\eta-\varepsilon}^{\eta} \frac{\epsilon^{x}}{x}\,dx$$

$$= \epsilon^{-\eta} I(\eta,\varepsilon)$$

$$= \epsilon^{-\eta}\left[\overline{Ei}(\eta) - \overline{Ei}(\eta-\varepsilon)\right] \qquad (2.16)$$

Figure 5 is a plot of $\overline{Ei}(x)$ obtained from values in Jahnke and Emde, Tables of Functions, pages 6-8. The values of x for which this function is plotted are those whose values are useful in equation (2.13) when used to predict the behavior of the capacitor of figure 1.

Figure 6 shows the expected behavior of the capacitor of figure 1 when placed in an RC series charging network. The shapes of these curves can be shown to be approximately correct for the circuit of figure 3 by allowing the voltage across the capacitor to vary from zero to approximately battery voltage for various battery voltages.

Charge Characteristics of Non-linear Capacitor

Solid – Charge
Dotted – Discharge

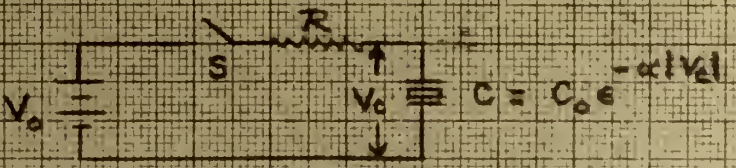

$\alpha V_o = 2$

$\alpha V_o = 1$

$\alpha V_o = 0.5$

Normalized Voltage Across Capacitor – αV_c $\frac{\text{Volts}}{\text{Volts}}$

2.0
1.8
1.6
1.4
1.2
1.0
0.8
0.6
0.4
0.2
0.0

0.0 0.50 1.0 1.5 2.0 2.5 3.0 3.5 4.0

Normalized Charge Time – $\frac{t}{RC_o}$ $\frac{\text{seconds}}{\text{seconds}}$

CHAPTER III

EXPERIMENTAL SWEEP FREQUENCY OSCILLATOR

Figure 7 shows the schematic diagram of an experimental radio frequency oscillator. This circuit will be recognized as that of a conventional Hartley oscillator circuit. Provision has been made at terminal "A" so that the D. C. voltage across the capacitors in the tank circuit may be varied. One capacitor is a 0.2 uf paper capacitor and the other capacitor is the barium titanate capacitor whose characteristics at 1000 cycles per second are shown in figure 1. Changing the voltage across the capacitors changes the capacity of the barium titanate capacitor and thus changes the resonant frequency of the tank circuit of the oscillator. The coil in the tank circuit has been chosen so that the resonant frequency of the tank will be near the intermediate frequencies used in conventional broadcast receivers.

Figure 8 shows the characteristics of a resonant circuit utilizing the capacitor of figure 1. Shown in the figure are the resonant frequencies as calculated from the 1000 cycle per second values of capacity and the resonant frequencies which were measured for the circuit. It is seen that the operation of the barium titanate capacitor at 350 to 650 kilocycles may be predicted approximately from measurements made at 1000 cycles.

Figure 9 shows the characteristics of the oscillator of figure 7. Shown in the figure is the experimental setup used to determine the characteristics. RMS values of the radio-frequency output voltage, experimental values of D. C. bias voltage required and D. C. bias

Figure 7

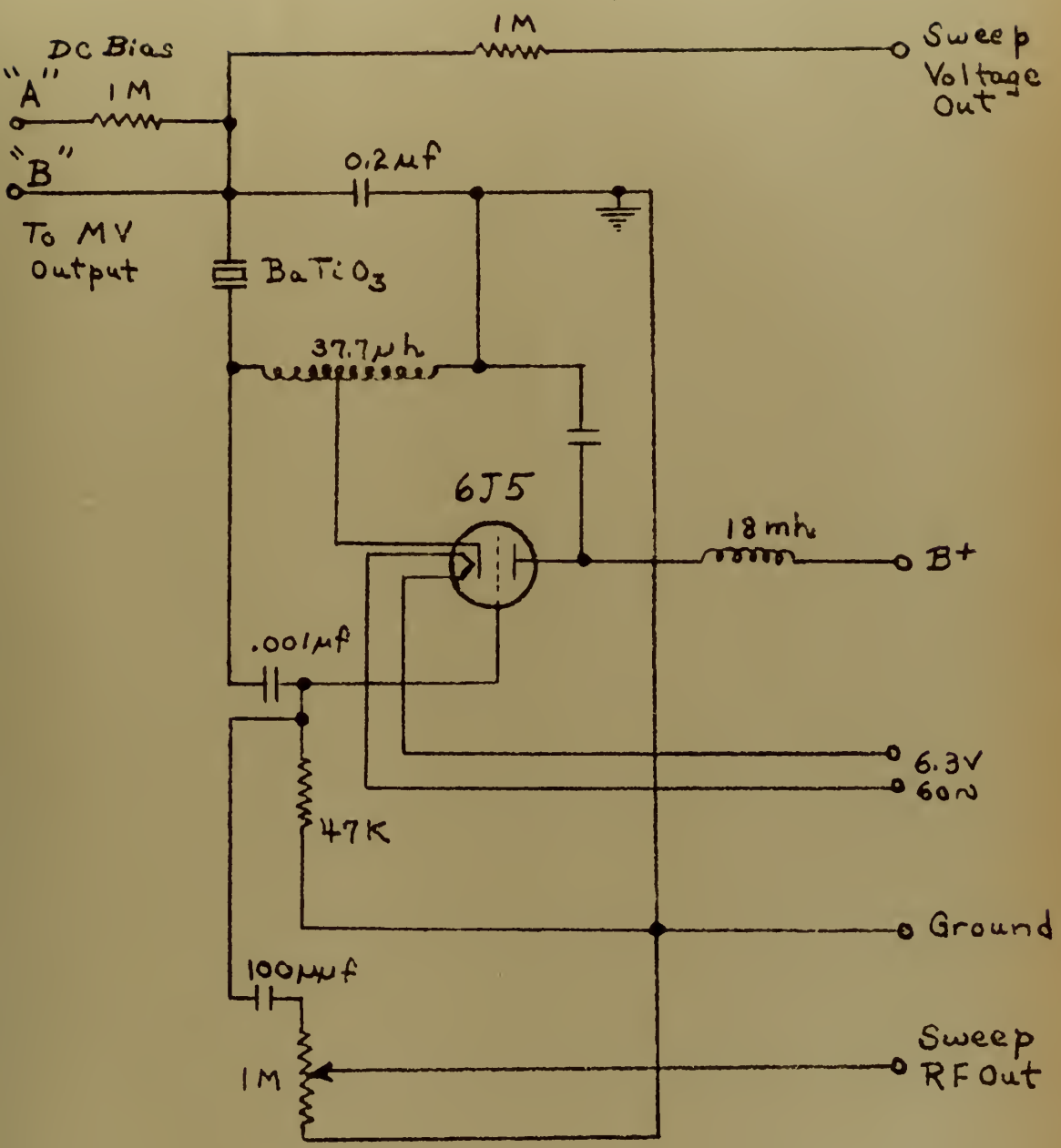

Sweep Frequency Oscillator

Figure 8


Series Resonant Circuit Using Barium Titanate Capacitor
Series Resonant Frequency - KCs
Calculated
Experimental
700
650
600
550
500
450
400
350
300
0
100
200
300
400
500
Bias Voltage
10Ω
40mH
0.1mF
0.5mH

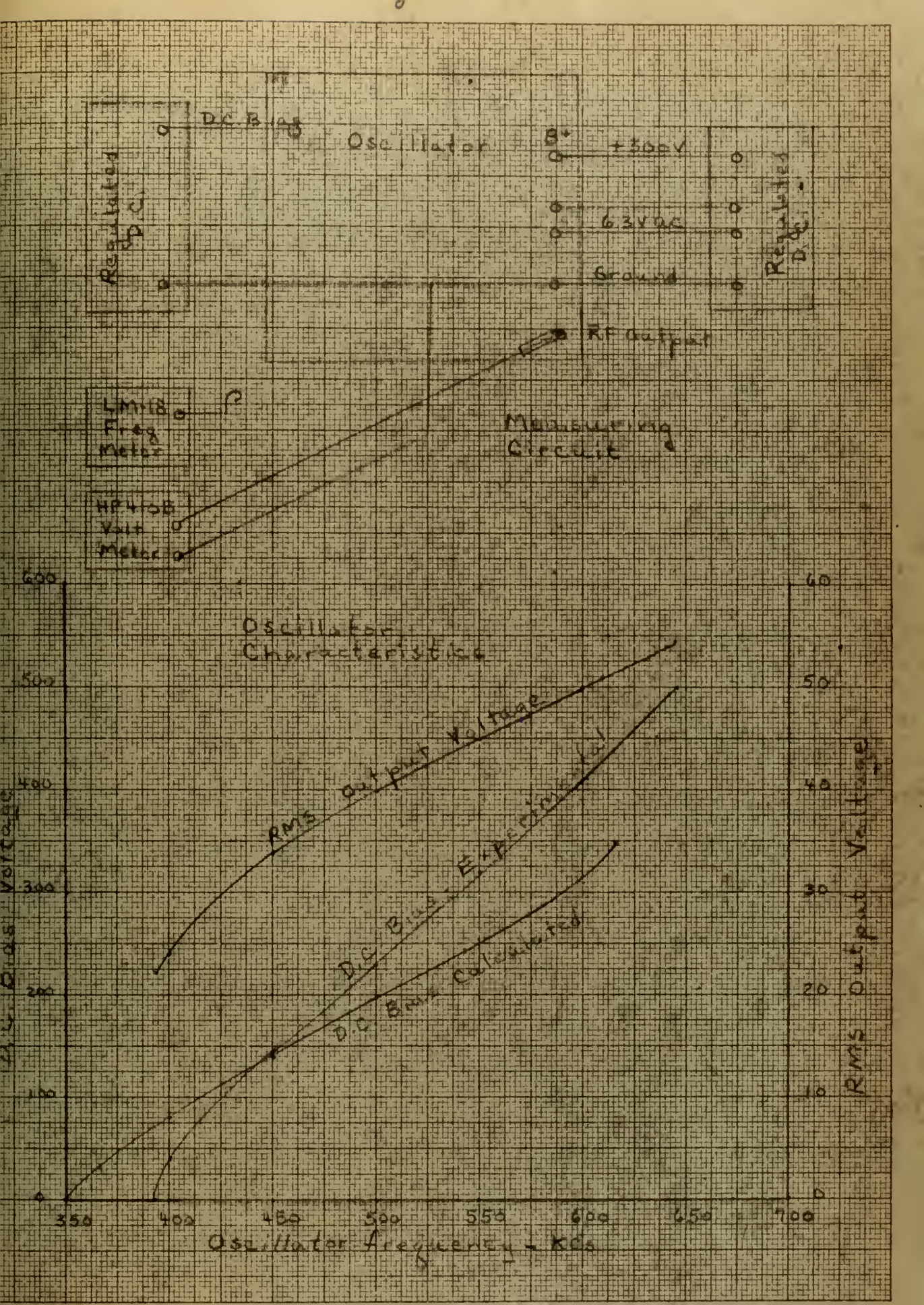
DC B
Oscillator
B+
+300V
63VAC
Ground
RF output
Measuring Circuit
Limiting Freq. Meter
HP410B Volt Meter
Oscillator Characteristics
RMS output Voltage
D.C. Bias + Rectified RF
D.C. Bias Calculated
Oscillator Frequency - KCs
RMS Output Voltage
D.C. Bias Voltage
350
400
450
500
550
600
650
700

calculated from 1000 cycles per second values of capacity are plotted against oscillator output frequency.

Figure 10 is the schematic diagram of an electron-coupled multivibrator. The output voltage of this circuit, when the output is connected to a resistive load, is a rectangular waveform of constant amplitude over wide variations in the value of R1 (Output Z Control) which does not affect the period of the rectangular wave. If an element Zx is placed across the output terminals of the multivibrator, the multivibrator then assumes the role of a switch which alternately connects Zx through R1 to B$\not$ for the time the output tube is cut-off, and then connects Zx to a low value of D. C. voltage when the output tube conducts heavily. Hence, if the multivibrator is connected to terminal "B" of the oscillator of figure 7, the bias voltage across the barium titanate capacitor may be varied and the frequency of the oscillator may be swept in time according to the manner in which the parallel combination of the barium titanate and the 0.2 uf paper capacitor charge through R1 toward B$\not$.

Figure 11 is a block diagram showing an experimental set-up in which the oscillator was used to check the frequency response curve of a conventional 456 kilocycle per second intermediate frequency amplifier and audio detector. In this set-up the center frequency of the oscillator is controlled by the adjustment of E1 which is a variable D. C. power supply and which sets the lowest bias voltage across the barium titanate capacitor during the sweep. The range of variation of frequency is controlled by the setting of the Output Z control on the multivibrator.

Figure 12 is a block diagram showing an experimental set-up used to

Figure 10

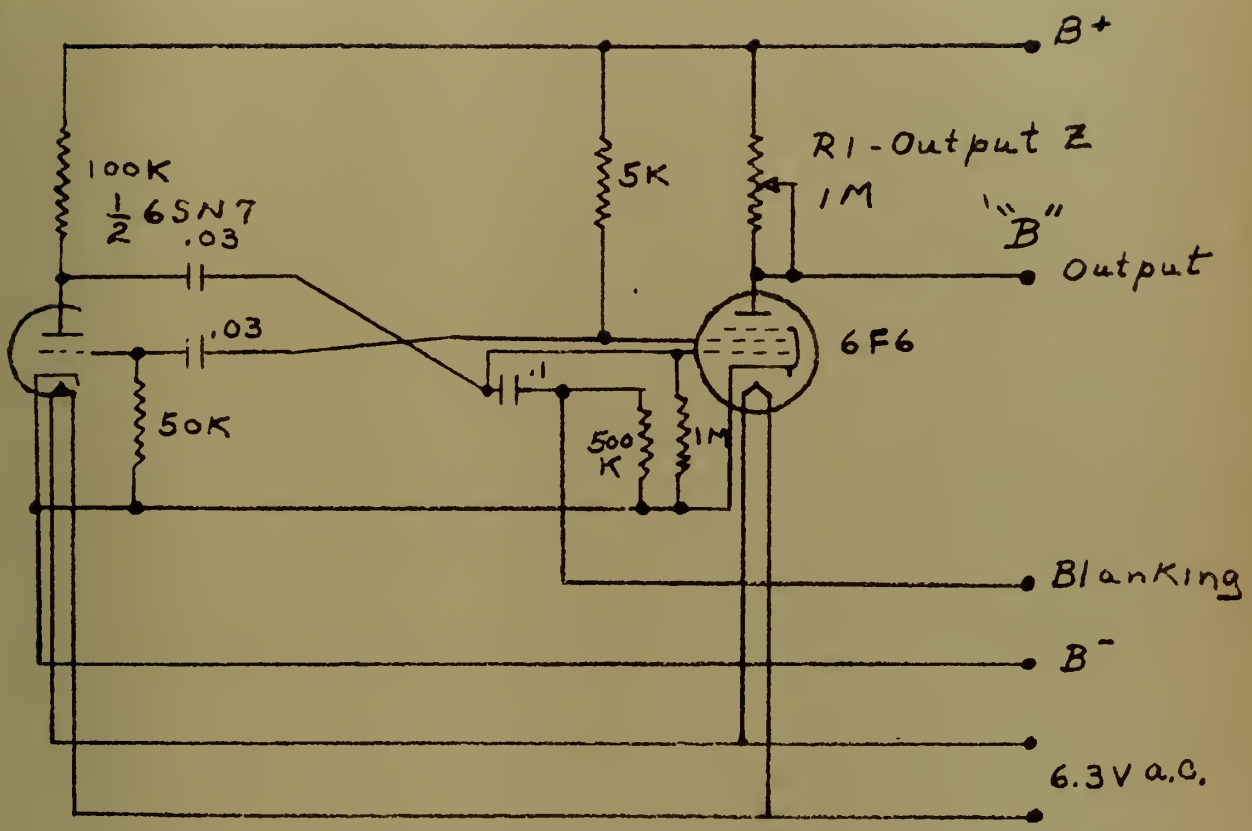

Electron - Coupled Multivibrator

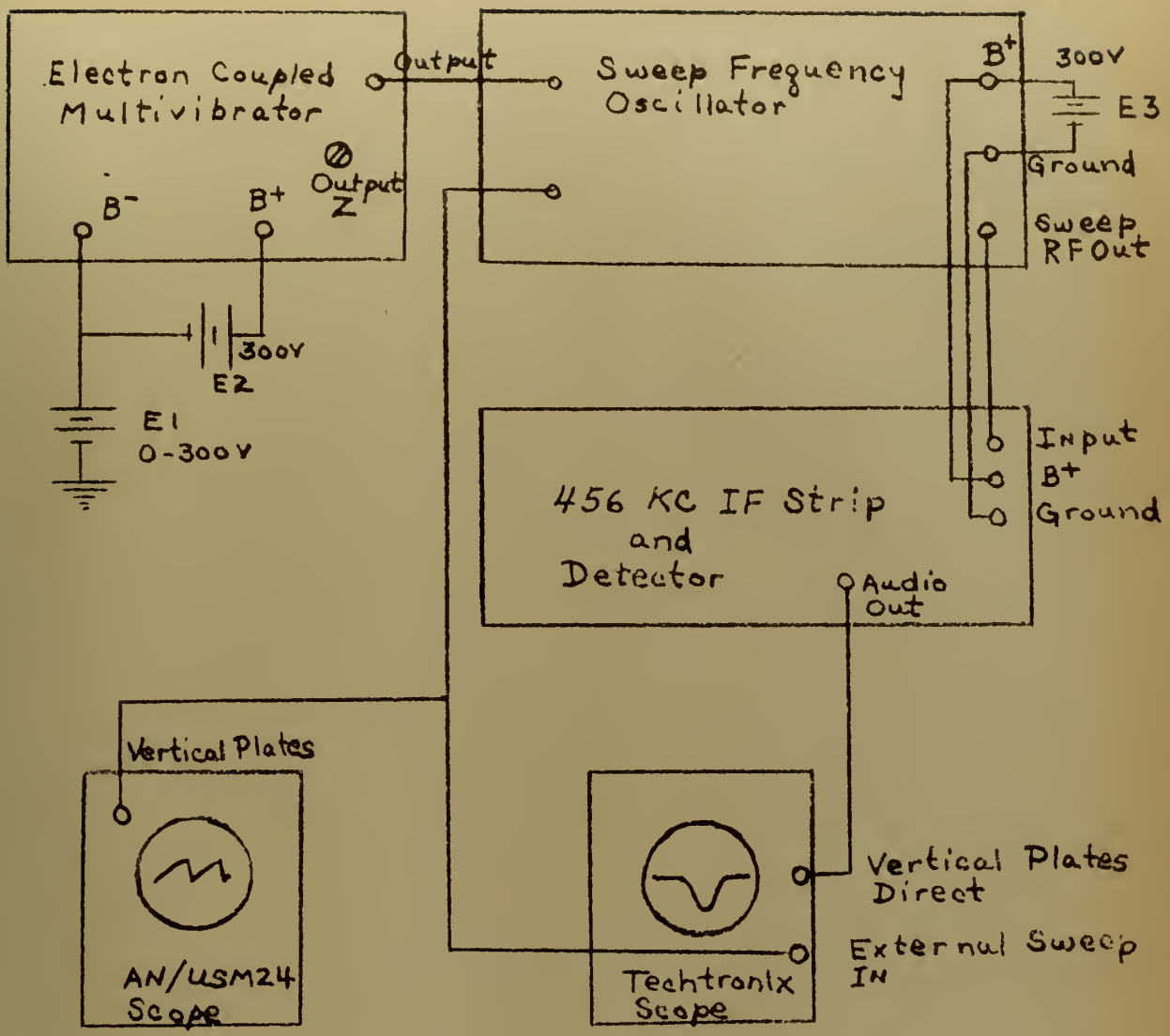

Figure 11 -Use of Sweep frequency Generator to Observe Response of 456-KC IF Strip

Center frequency controlled by E1

Frequency Sweep width Controlled by Output Z of multivibrator

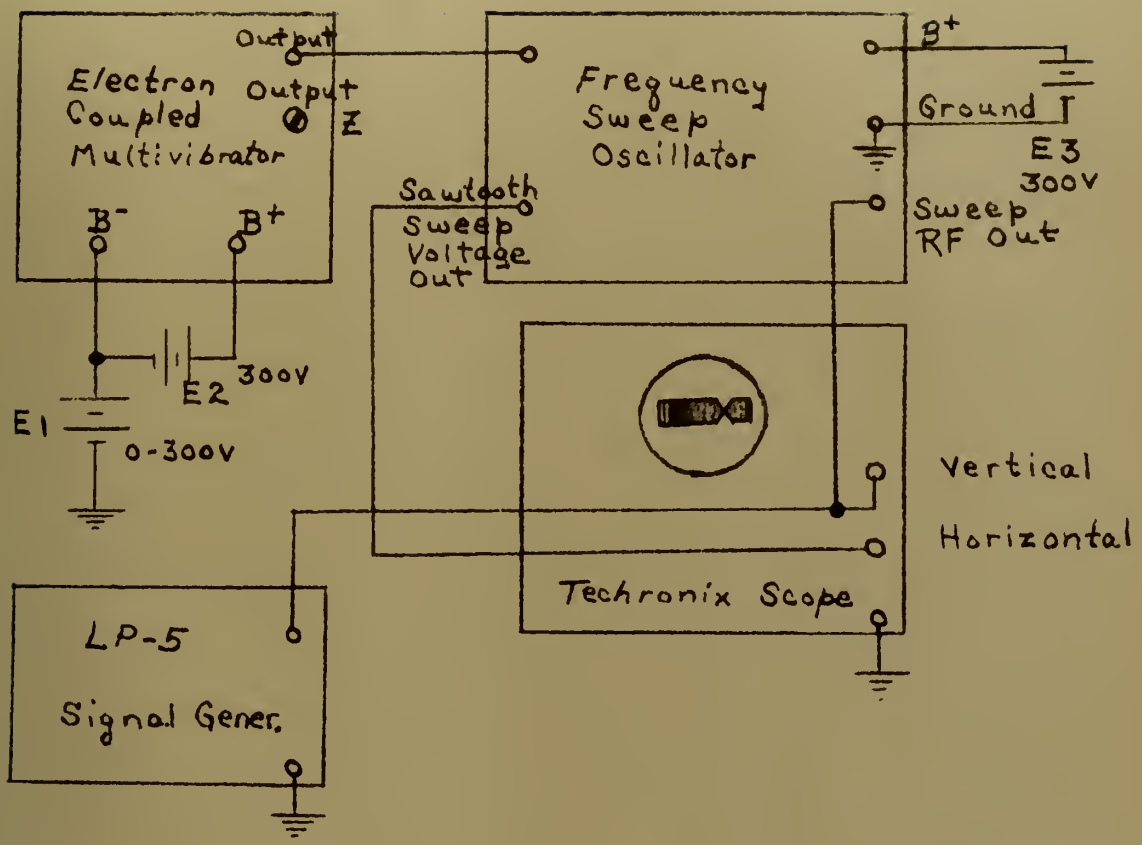

Figure 12 - Circuit for determining the dynamic range of the sweep frequency RF Oscillator

determine the dynamic range of the oscillator of figure 7. The Navy Model LP-5 signal generator is beat against the swept frequency output of the oscillator. At the time that the two frequencies are equal, zero-beat is obtained and a notch shows up in the pattern on the oscilloscope. The horizontal sweep voltage applied to the oscilloscope is derived from the same voltage which is across the barium titanate capacitor in the oscillator. By varying the frequency of the LP-5 the notch may be moved from the left to the right extreme edges of the pattern on the oscilloscope and the dynamic range of frequencies swept measured.

While the circuit of figure 7 provides a simple and inexpensive swept frequency oscillator which illustrates the advantages Barium Titanate has over a reactance tube circuit as to simplicity and wide range, this circuit does not utilize fully the advantages which may be gained by the use of Barium Titanate. In this simple circuit the center frequency control interacts with the swept frequency width control; the amplitude of the RF output voltage increases considerably with frequency; and to ensure that the spectrum of a device, whose input is the output of the above swept frequency oscillator, is properly interpreted, the sweep output voltage of the swept frequency oscillator must be used for the x-axis voltage of the monitoring oscilloscope. As will be shown in a later circuit the above disadvantages may be practically eliminated by replacing the standard 0.2 uf capacitor of figure 7 with another barium titanate capacitor accompanied with some rearrangement of the D. C. voltage supplies and switching circuitry.

Figure 13 shows a more elaborate swept frequency generator. In this generator the center frequency control and the swept frequency width

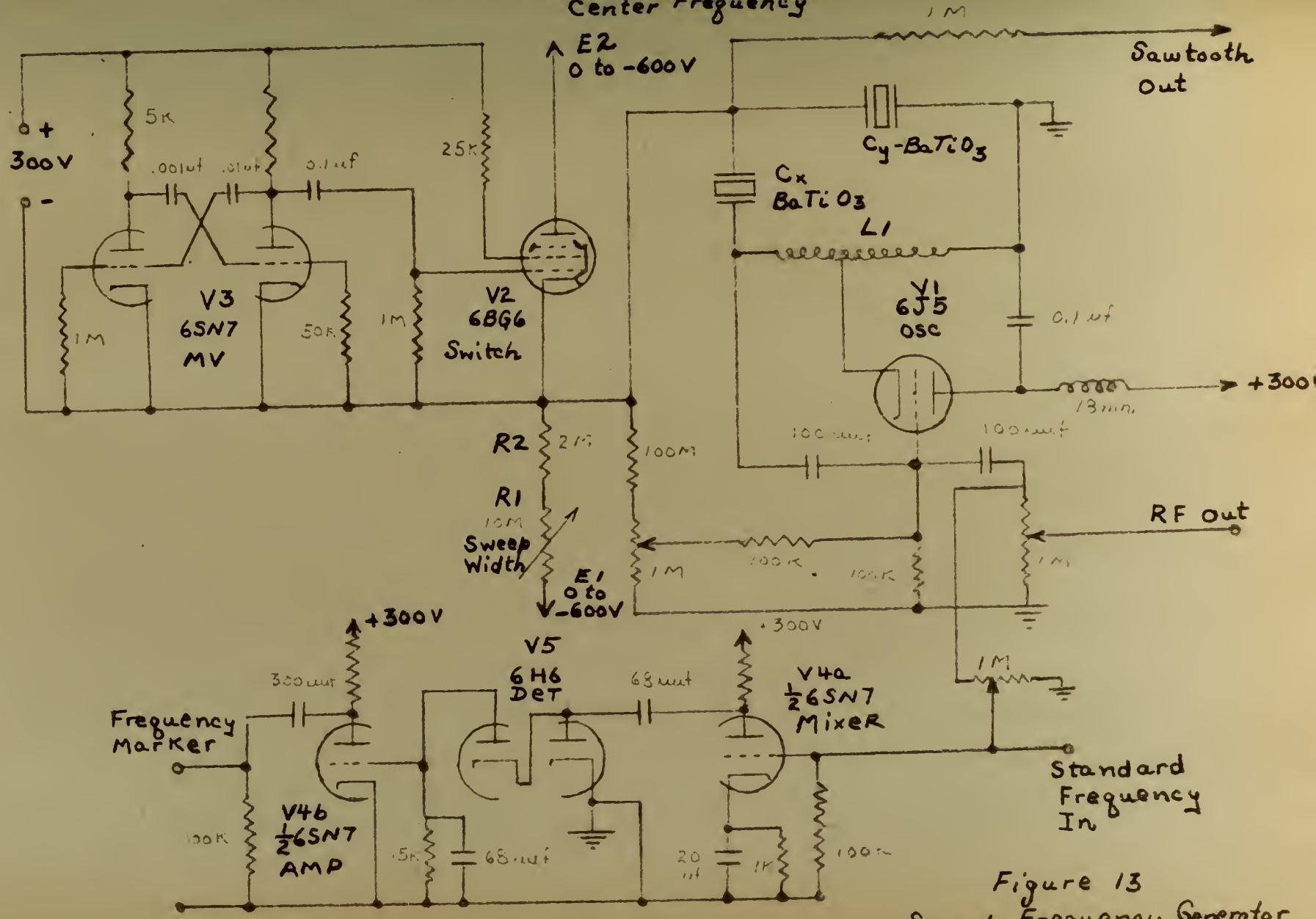

Figure 13
Swept Frequency Generator

controls are relatively independent; the frequency of the output voltage approximates a linear function of time which will be shown later to have two advantages in a generator of this type; the amplitude is flatter over the entire range of frequencies than for the simple generator of figure 7; and a frequency marker is provided.

The circuit of figure 13 operates as a conventional Hartley oscillator. The frequency determining tank consists of the coil L_1, capacitor C_x and C_y, in series. C_x and C_y are two similar capacitors made from type K-6000 Barium Titanate. The instantaneous frequency of the oscillator is determined by the instantaneous bias voltage across the individual Barium Titanate capacitors.

The Barium Titanate capacitors, C_x and C_y, serve several purposes in the circuit of figure 13. The series capacity of C_x and C_y determines the frequency of the oscillator, V1. C_x and C_y, in parallel, also are actually part of the charging network which determines the bias voltage wave form which tunes the oscillator. The peculiar charging characteristic of these nonlinear capacitors is utilized here to form a voltage wave form which changes the capacity of the Barium Titanate capacitors in such a way that the output frequency of the oscillator approximates a linear function of the time over the total range of the oscillator. Also the charging network is so arranged that the wave form developed by C_x and C_y, which is a negative voltage wave form whose amplitude becomes more negative with time and frequency, can be used to reduce the variations of output voltage with output frequency.

Figures 14(a) and 15(a) show the variation in bias voltage across C_x and C_y, in parallel, as a function of time for D. C. charging voltage

Figure 14

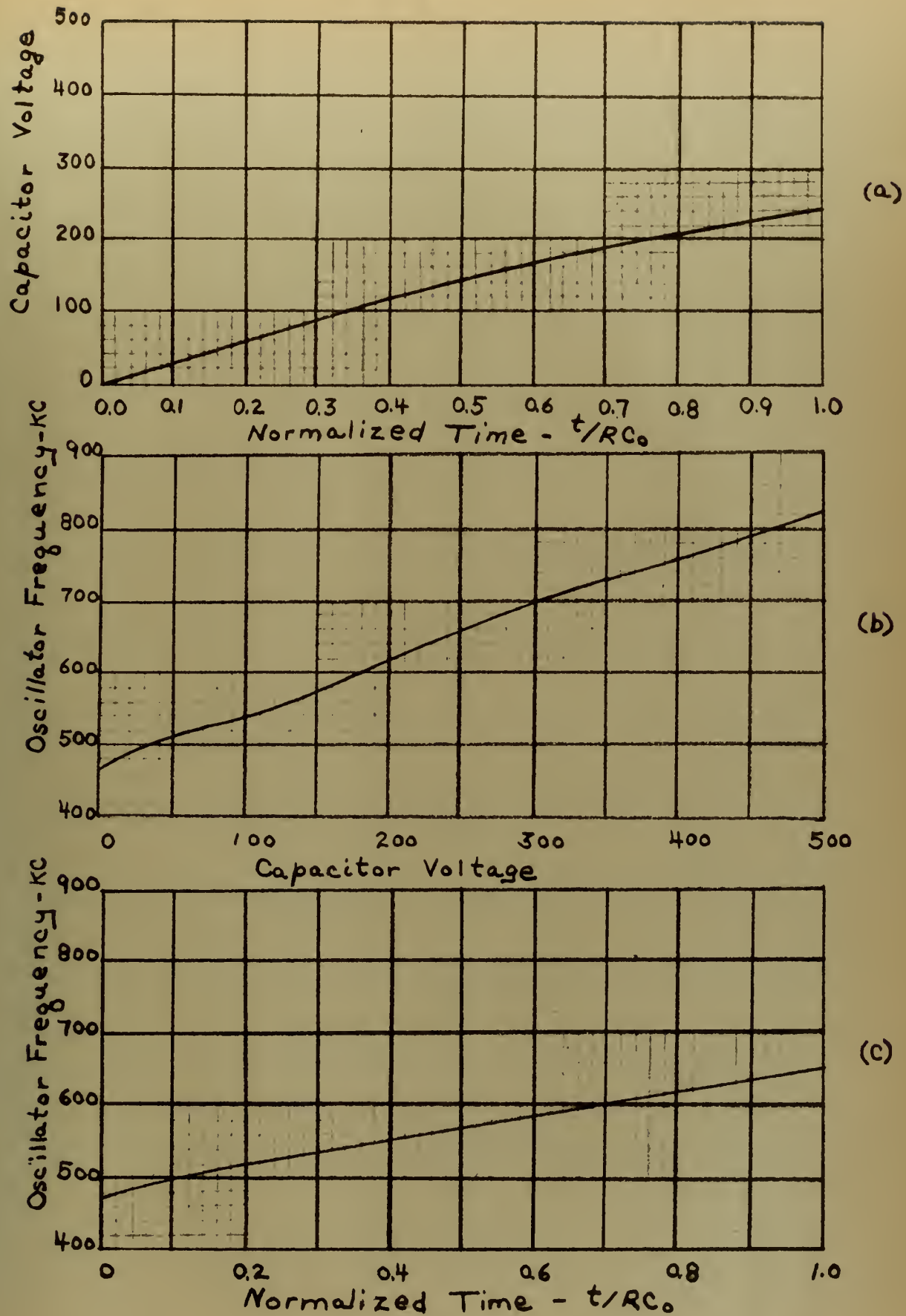

Characteristics of Swept Frequency Generator
300 - Volt Supply

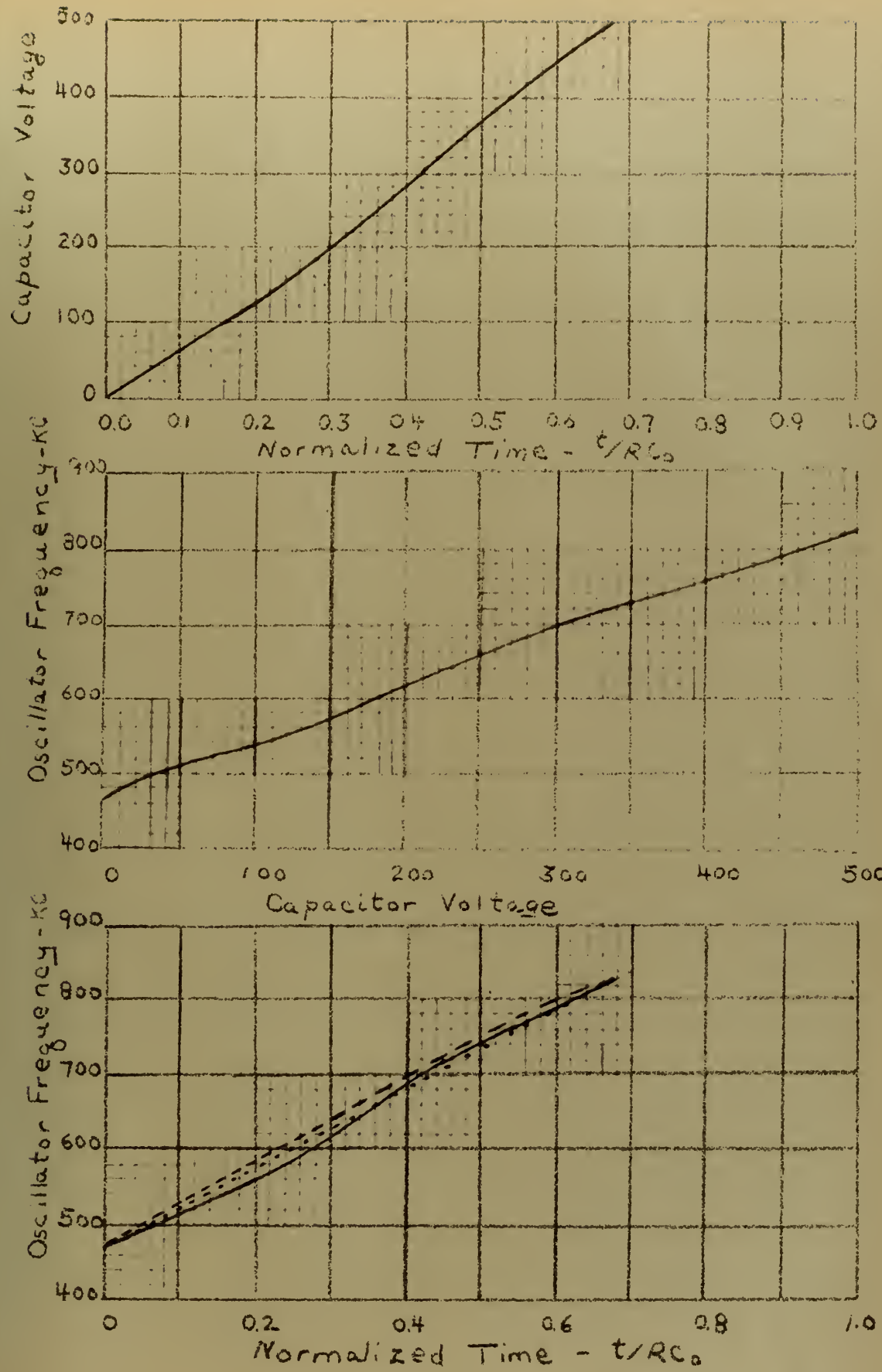

Characteristics of Swept Frequency Generator
600 - Volt Supply

supplies of 300-volts and 600-volts, respectively. It will be noted that the voltage wave form is similar to that expected for the charge of the capacitor of figure 1. The difference lies in the effective value of α which for this circuit has a value of 1/300-volts as determined from oscilloscope patterns instead of the value of 1/260-volts determined from the curve of figure 1.

Figures 14(b) and 15(b) show the variation in oscillator frequency as a function of bias voltage across the Barium Titanate capacitors. It will be noted that the frequency is more linear with variations in bias voltage than is predicted by the simple relation of equation (2.02) for the capacity as a function of bias voltage.

Figure 14(c) shows the variation of frequency with time for the swept frequency oscillator using two barium titanate capacitors and a charging voltage of 300-volts. It is noted that the wave form of voltage produced by the Barium Titanate capacitors in this case is the same as would be produced by replacing C_x with a conventional capacitor but with a charging voltage of 450-volts. Figure 15(c) shows the variation of frequency with time for the swept frequency oscillator using two Barium Titanate capacitors and a charging voltage of 600-volts. Also shown by the dashed line in figure 15(c) is the computed variation of frequency with time for the swept frequency oscillator utilizing one Barium Titanate capacitor and one conventional capacitor with a supply voltage of 1270 volts. It can be seen that in so far as linear variation of frequency with time is concerned the 600-volt supply is equivalent, when used with two barium titanate capacitors, to the 1270-volt supply when used with one barium titanate and one conventional capacitor. It is thus

an advantage to use two barium titanate capacitors in this circuit since it allows a considerable reduction of the magnitude of the D. C. voltage supply required.

There are two advantages to be gained by making the frequency output a linear function of time. An important advantage in operation of the generator is that it makes the swept frequency width control independent of the center frequency control if the time allowed per sweep is held constant as is the case in this circuit. Another advantage lies in the fact that over a wide range it is no longer absolutely required that the bias voltage across the capacitors be used for the x-axis voltage of a monitoring oscilloscope to observe the spectrum of the device under measurement. In this case the oscilloscope's internal linear sawtooth voltage may be used satisfactorily in spectrum analysis.

Auxiliary circuits include a timing multivibrator, V3; switch tube, V2; mixer, V4a; detector, V5; and pulse amplifier, V4b.

V3 is a conventional free-running multivibrator whose output is used to turn on and to cut off the switch tube, V2. Circuit parameters are so chosen that V2 is cut off for a much longer time than it is allowed to conduct.

The purpose of V2 is to switch the barium titanate capacitors from the equivalent D. C. circuit of figure 16(a) to the equivalent D. C. circuit of figure 16(b). In figure 16(a) the switch tube V2 is cut off and the barium titanate capacitors charge from an initial value toward E1. The rate of charge is determined by R1, Sweep Frequency Width Control. The final value of the voltage across the barium titanate capacitors is determined by how long V2 is allowed to remain cut off. In figure 16(b),

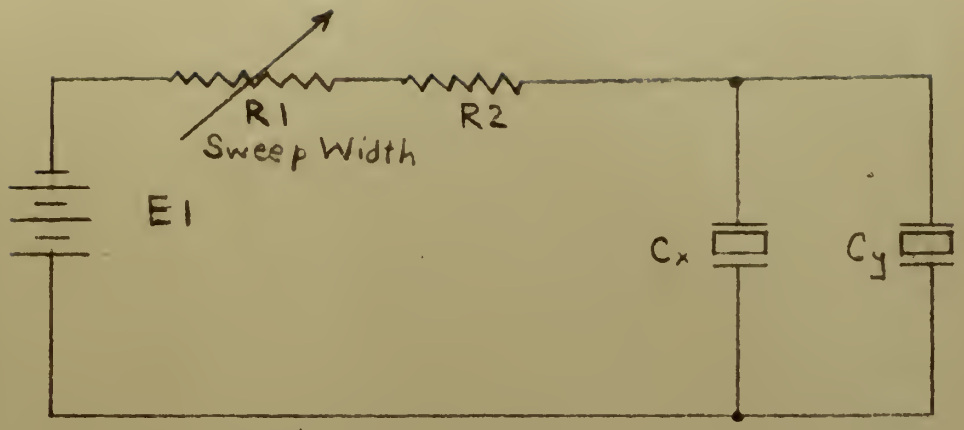

(a) Charge Circuit

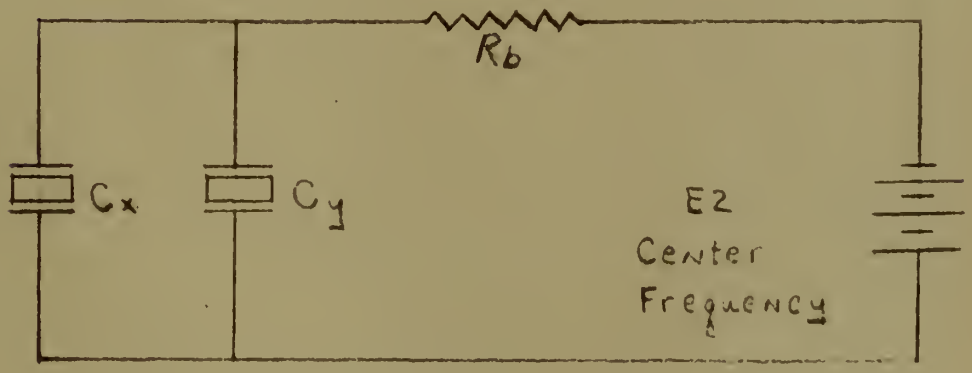

(b) Discharge Circuit

Figure 16 - Charge and Discharge Circuits in Swept Frequency Generator

V2 is turned on and the barium titanate capacitors are allowed to discharge. The conducting resistance of V2 is very much lower than R1 plus R2 and hence the equivalent circuit for discharge of the barium titanate capacitors is that shown in 16(b) so long as the magnitude of E2 is much lower than E1. Since the value of voltage across the barium titanate capacitors varies from a value near E2 to a higher value determined by R1 during each sweep, E2 serves as the Center Frequency Control and R1 serves as the Sweep Frequency Width Control. Since the slope of the curves of figures 14(c) and 15(c) are approximately constant with time and the amount of time allowed per sweep is constant, the Sweep Frequency Width Control and the Center Frequency Control are relatively independent.

In figure 13, V4a serves as a mixer to combine the swept frequency output of V1 with the output of a standard signal generator such as the Navy Model LP-5. The wave form at the plate of V4a is similar to the wave form shown on the oscilloscope face in figure 12. The notch in the wave form occurs when the frequency of V1 is instantaneously equal to the frequency of the standard fixed frequency. This wave form is applied to V5 which is an envelope detector and the output of the detector is applied to the grid of the amplifier V4b. V4b is held cut off until the notch in the wave form occurs at which time V4b conducts. The output of V4b is a negative pulse which occurs when the frequency of V1 is instantaneously equal to the standard frequency so that the pulse may be applied to the z-axis of a monitoring oscilloscope to serve as a frequency marker.

It was anticipated that the frequency drift in the oscillators shown in figures 7 and 13 due to variations in room temperature would not be

significant since variations in frequency of a swept frequency generator are made intentionally large. No attempt was then made to stabilize the oscillators by placing the barium titanate capacitors in temperature controlled atmospheres as must be done in fixed frequency applications. In making the measurements which are illustrated in figure 9, it was found that the frequency difference was approximately 1 kilocycle per second between normal room temperature with no forced draft and the temperature resulting from placing a forced draft blower near the barium titanate. This is not considered significant in the application illustrated in figure 11 where the normal width of the swept frequency was about 25 kilocycles per second.

It was not known how the frequency of the oscillators would change with ageing of the barium titanate. However, in the experimental set-up illustrated in figure 12, it was found that no significant changes had occurred over a period of approximately three months. It was found that the peak to peak voltage of the sawtooth voltage across the barium titanate could be determined within 1% from the measurements of E1 and the frequency of the LP-5 Signal Generator when the measurements were referred to the curve of figure 9 which had been made three months earlier. As pointed out in the recent article by Mason and Wick [4] and Shaw and Jenkins [5], much work is being done in the field to stabilize the electrical characteristics of barium titanate which should eliminate changes due to ageing of the dielectric.

Measurements made in connection with the experimental oscillators described in this paper indicate that barium titanate nonlinear capacitor control of a swept frequency oscillator is feasible and that no serious

difficulties are presented in the design of this type circuit using barium titanate capacitors.

BIBLIOGRAPHY

1. Apstein, Maurice and H. H. Wieder — CAPACITOR-MODULATED WIDE-RANGE FM SYSTEM
Electronics, October 1953

2. Dranetz, A. I., Howatt, G. N., and Crownover — BARIUM TITANATES AS CIRCUIT ELEMENTS
Tele-Tech, Three Parts
Part I, April 1949
Part II, May 1949
Part III, June 1949

3. MacDonald, J. R. and Brachman, M. K. — THE CHARGING AND DISCHARGING OF NONLINEAR CAPACITORS
Proc. I.R.E., January 1955

4. Mason, W. P. and Wick, R. F. — FERROELECTRICS AND THE DIELECTRIC AMPLIFIER
Proc. I.R.E., November 1954

5. Shaw, G. S. and Jenkins, J. L. — NONLINEAR CAPACITORS FOR DIELECTRIC AMPLIFIERS
Electronics, October 1953

6. Von Hippel, A. R. — DIELECTRICS AND WAVES
John Wiley and Sons (1954)
New York, New York

DERIVATION OF EQUATIONS OF CHARGE OF A NON-LINEAR CAPACITOR WHOSE CAPACITY AS A FUNCTION OF VOLTAGE VARIES AS $C_o - kV_c$:

In figure 2 are shown a charging circuit consisting of a capacitor and a resistor in series with a battery, V_o. The resistor is assumed to be of constant value and independent of voltage. The capacitor is assumed to have the characteristics shown above the circuit as $C = C_o(1 - Vc/Vm)$:

The differential equation for the charging current is:

$$i = \frac{V_o - V_c}{R} = C\frac{dV_c}{dt} = \left(C_o - \frac{C_o}{V_m}V_c\right)\frac{dV_c}{dt} \tag{1}$$

$$= (C_o - KV_c)\frac{dV_c}{dt} \tag{2}$$

$$\therefore dt = \frac{R(C_o - KV_c)}{V_o - V_c}dV_c \tag{3}$$

$$\therefore \int_{t_1}^{t} dt = R\int_{V_1}^{V_c}\frac{C_o - KV_c}{V_o - V_c}dV_c \tag{4}$$

$$\therefore t - t_1 = RK\int_{V_1}^{V_c} dV_c + R\int_{V_1}^{V_c}\frac{C_o - KV_o}{V_o - V_c}dV_c \tag{5}$$

if: $t_1 = o$ and $x = V_o - V_c$ (6)

$$dx = -dV_c$$

$$\frac{dx}{x} = -\frac{dV_c}{V_o - V_c}$$

when: $V_c = V_1$, $x = V_o - V_1$

$V_c = V_c$, $x = V_o - V_c$

$$t = RK'(V_c - V_1) + R(C_o - KV_o)\int_{V_o - V_c}^{V_o - V_1} \frac{dx}{x} \tag{7}$$

$$t = RK(V_c - V_1) + R(C_o - KV_o)\ln\frac{V_o - V_1}{V_o - V_c} \tag{8}$$

$$\therefore \quad t = RC_o\left(\frac{V_c - V_1}{V_m}\right) + RC_o\left(1 - \frac{V_o}{V_m}\right)\ln\frac{V_o - V_1}{V_o - V_c} \tag{9}$$

$$\therefore \quad \frac{t}{RC_o} = \frac{V_c - V_1}{V_m} + \left(1 + \frac{V_o}{V_m}\right)\ln\frac{V_o - V_1}{V_o - V_c} \tag{10}$$

where: V_1 = voltage across the capacitor at t = 0

V_c = voltage across the capacitor at any time - t

Vm = intercept on the Vc - axis

Co = intercept on the C- axis

In the special case where $V_o = V_m$, equation (10), above reduces to a linear equation:

$$\frac{t}{RC_o} = \frac{V_c - V_1}{V_m} \tag{11}$$

$$V_c = V_1 + V_m\frac{t}{RC_o} \tag{12}$$

APPENDIX II

DERIVATION OF THE EQUATIONS OF CHARGE AND DISCHARGE OF A NON-LINEAR CAPACITOR WHOSE CAPACITY AS A FUNCTION OF VOLTAGE VARIES AS A NEGATIVE EXPONENTIAL

It is assumed that the capacitor shown in the series charging circuit of figure 6 varies as:

$$C = C_o + C_1 \epsilon^{-\alpha V_c} \tag{1}$$

If at t = 0, the switch S is suddenly closed and the voltage across the capacitor is initially zero:

$$i = \frac{V_o - V_c}{R} = \left(C_o + C_1 \epsilon^{-\alpha V_c}\right) \frac{dV_c}{dt} \tag{2}$$

$$R\left(C_o + C_1 \epsilon^{-\alpha V_c}\right) \frac{dV_c}{dt} = V_o - V_c \tag{3}$$

$$dt = \frac{R\left(C_o + C_1 \epsilon^{-\alpha V_c}\right)}{V_o - V_c} dV_c \tag{4}$$

$$\int_0^t dt = \int_0^{V_c} \frac{R C_o}{V_o - V_c} + R C_1 \int_0^{V_c} \frac{\epsilon^{-\alpha V_c}}{V_o - V_c} dV_c \tag{5}$$

if: $$\chi = \alpha (V_o - V_c) \tag{6}$$

$$d\chi = -\alpha V_c$$

when: $V_c = 0$, $\chi = \alpha V_o$

$V_c = V_c$, $\chi = \alpha (V_o - V_c)$

$$t = RC_o \int_{\alpha(V_o - V_c)}^{\alpha V_o} \frac{dx}{x} + RC_1 \epsilon^{-\alpha V_o} \int_{\alpha(V_o - V_c)}^{\alpha V_o} \frac{\epsilon^x}{x} dx \qquad (7)$$

$$t = RC_o \ln \frac{\alpha V_o}{\alpha(V_o - V_c)} + RC_1 \epsilon^{-\alpha V_o} \int_{\alpha(V_o - V_c)}^{\alpha V_o} \left\{ \frac{1}{x} \sum_{n=0}^{\infty} \frac{x^n}{n!} \right\} dx \qquad (8)$$

$$t = RC_o \ln \frac{\alpha V_o}{\alpha(V_o - V_c)} + \left| \ln x + \sum_{n=1}^{\infty} \frac{x^n}{n \cdot n!} \right|_{\alpha(V_o - V_c)}^{\alpha V_o} RC_1 \epsilon^{-\alpha V_o} \qquad (9)$$

From: Jahnke and Emde - pgs 1-8

$$\mathfrak{G}_i[x] = \sum_{n=1}^{\infty} \frac{x^n}{n \cdot n!} \qquad (10)$$

(Summed over all odd n's)

$$\mathfrak{C}_i[x] = \sum_{n=2}^{\infty} \frac{x^n}{n \cdot n!} + \ln \gamma x \qquad (11)$$

(Summed over all even n's)

$$\overline{E_i}[x] = \mathfrak{G}_i[x] + \mathfrak{C}_i[x] \qquad (12)$$

$$= \ln \gamma x + \sum_{n=1}^{\infty} \frac{x^n}{n \cdot n!} \qquad (13)$$

(Summed over all values of n)

$$\overline{Ei}[\alpha V_o] - \overline{Ei}[\alpha(V_o - V_c)] = \ln \sigma \alpha V_o + \sum_{n=1}^{\infty} \frac{(\alpha V_o)^n}{n \cdot n!}$$

$$- \ln \sigma \alpha (V_o - V_c) - \sum_{n=1}^{\infty} \frac{[\alpha (V_o - V_c)]^n}{n \cdot n!} \qquad (14)$$

$$= \ln \frac{\alpha V_o}{\alpha (V_o - V_c)} + \sum_{n=1}^{\infty} \frac{(\alpha V_o)^n}{n \cdot n!} - \sum_{n=1}^{\infty} \frac{[\alpha (V_o - V_c)]^n}{n \cdot n!} \qquad (15)$$

$$= \left| \ln x + \sum_{n=1}^{\infty} \frac{x^n}{n \cdot n!} \right|_{\alpha (V_o - V_c)}^{\alpha V_o} \qquad (16)$$

$$\therefore t = RC_o \ln \frac{\alpha V_o}{\alpha (V_o - V_c)} + RC_1 \epsilon^{-\alpha V_o} \left\{ \overline{Ei}[\alpha V_o] - \overline{Ei}[\alpha (V_o - V_c)] \right\} \qquad (17)$$

The values of $\overline{Ei}(x)$ are tabulated in JAHNKE AND EMDE Pages 6-8.

For the discharge of the nonlinear capacitor it is assumed that at time, $t = 0$, the voltage across the capacitor is equal to V_o and that the battery is suddenly removed and replaced by a short circuit. The following equations describe the expected behavior of the circuit:

$$C = C_o + C_1 \epsilon^{-\alpha V_c} \qquad (18)$$

$$-\frac{V_c}{R} = i = C\frac{dV_c}{dt} = \left(C_0 + C_1 \epsilon^{-\alpha V_c}\right)\frac{dV_c}{dt} \tag{19}$$

$$-\int_0^t dt = RC_0\int_{V_0}^{V_c}\frac{dV_c}{V_c} + RC_1\int_{V_0}^{V_c}\frac{\epsilon^{-\alpha V_c}}{V_c}\,dV_c \tag{20}$$

$$-t = RC_0 \ln\frac{V_c}{V_0} + RC_1\left[\int_{\alpha V_0}^{\infty}\frac{\epsilon^{-x}}{x}dx - \int_{\alpha V_c}^{\infty}\frac{\epsilon^{-x}}{x}dx\right] \tag{21}$$

therefore:

$$t = RC_0 \ln\frac{V_0}{V_c} + \left[Ei(-\alpha V_0) - Ei(-\alpha V_c)\right]RC_1 \tag{22}$$

where:

$$-Ei(-x) = \int_x^{\infty}\frac{\epsilon^{-t}}{t}dt \quad > 0\,,\ \infty > x > 0 \tag{23}$$

Numerical values of Ei (-x) may be found in Jahnke and Emde, "Tables of Functions".